Available online at www.sciencedirect.com

ScienceDirect

www.elsevier.com/locate/jes

JES JOURNAL OF ENVIRONMENTAL SCIENCES

www.jesc.ac.cn

Simultaneous removal of gaseous CO and elemental mercury over Cu-Co modified activated coke at low temperature

Fengyu Gao[1,2], *Hao Yan*[1], *Xiaolong Tang*[1,2,*], *Honghong Yi*[1,2], *Shunzheng Zhao*[1,2], *Qingjun Yu*[1,2], *Shuquan Ni*[1]

[1] *School of Energy and Environmental Engineering, University of Science and Technology Beijing, Beijing 100083, China*

[2] *Beijing Key Laboratory of Resource-oriented Treatment of Industrial Pollutants, University of Science and Technology Beijing, Beijing 100083, China*

ARTICLE INFO

Article history:
Received 9 March 2020
Revised 25 May 2020
Accepted 27 May 2020
Available online 21 August 2020

Keywords:
Synergetic catalysis
Cu-Co oxides
Carbon monoxide
Element mercury
Activated coke

ABSTRACT

Cu-Co multiple-oxides modified on HNO_3-pretreated activated coke (AC_N) were optimized for the simultaneous removal of gaseous CO and elemental mercury (Hg^0) at low temperature (< 200 °C). It was found that 2%CuOx-10%CoOx/AC_N catalyst calcined at 400°C resulted in the coexistence of complex oxides including CuO, Cu_2O, Co_3O_4, Co_2O_3 and CoO phases, which might be good for the simultaneous catalytic oxidation of CO by Co-species and removal of Hg^0 by Cu-species, benefiting from the synergistic catalysis during the electro-interaction between Co and Cu cations ($CoO \rightleftharpoons Co_3O_4$ and $Cu_2O \rightleftharpoons CuO$). The catalysis removal of CO oxidation was obviously depended on the reaction temperature obtaining 94.7% at 200 °C, while no obvious promoting effect on the Hg^0 removal (68.3%-78.7%). These materials were very substitute for the removal of CO and Hg° from the flue gas with the conditions of 8–20 vol.% O_2 and flue-gas temperature below 200 °C. The removal of Hg° followed the combination processes of adsorption and catalytic oxidation reaction via Langmuir-Hinshelwood mechanism, while the catalysis of CO abided by the Mars-van Krevelen mechanism with lattice oxygen species.

Introduction

Clean atmosphere is one of the essentials for the beautiful ecological environment and green-to-blue livable cities. In the iron-steel, independent and affiliated coke-oven industries, it has caused a worldwide concern on the removal of gaseous carbon monoxide (CO) and heavy metal mercury (Hg) with a large contents, which are with high levels of toxicity, bio-accumulation, and persistence (Wang et al., 2016; Xu et al., 2017). For instance, sintering flue gas emits gaseous CO with a large content of about 0.5–1.0 vol.% and contributes to about 41% of the total atmospheric mercury emissions in China (Hg emission factor is about 1.28–2.49 mg/ton sinter and the average emission concentration is 17.8–31.8 μg/m^3). Efficient and stable catalysts are of great importance for the purification of gaseous pollutants from industrial flue gases. Nowadays, adsorption and catalysis coupling techniques have become the

* Corresponding author.
E-mail: txiaolong@126.com (X. Tang).

https://doi.org/10.1016/j.jes.2020.05.029

collaborative purification technology of comparative advantage by using multifunctional materials.

The elemental mercury (Hg^0), oxidized mercury (Hg^{2+}) and particulate-bound mercury (Hg^p) are the main existing forms of mercury in flue gas (Jew et al., 2015). The latter two forms (Hg^{2+} and Hg^p) can be controlled by the existing flue gas purification system (Fu et al., 2016). However, elemental mercury has high stability and low solubility, which is a problem for the effective removal of Hg^0 (Zhao et al., 2016). It is a potential technology to removal the elemental mercury by the catalytic oxidation to Hg^{2+}. As presented in the report (López-Antón et al., 2016), the selective catalytic reduction (SCR) of NOx worked at the temperature range of 300–400 °C has a certain catalytic oxidation effect on elemental mercury (Hg^0). Chi et al. (2017) found that 7%Ce-1%CuOx modified V_2O_5/TiO_2 SCR catalyst exhibited the highest NO conversion efficiency (>97%) at 200–400 °C, as well as the best Hg^0 oxidation activity (>75%) at 150–350 °C. In our previous studies (Zhao et al., 2016; Zhao et al., 2019), we found that 8 wt.% loading value of CuO over activated coke (AC) was found to be the optimal material for mercury removal achieving around 73% average efficiency at 120°C, and that further optimized 8%Cu-5%MnOx/AC obtained superior removal efficiency of mercury (>90%) and NOx by SCR (78%), simultaneously. Nowadays, the catalytic oxidation materials had been widely investigated to remove Hg^0 more effectively. Transition metals (Fe (Han et al., 2016; Huang et al., 2016), Ce (He et al., 2016; Li et al., 2017), Mn (Cimino and Scala, 2016; Guo et al., 2012; Jampaiah et al., 2016) and Cu (Zhao et al., 2016), etc.) had been shown a certain of catalytic activity for the oxidation of elemental mercury. Supporters such as activated carbon or coke (AC) (Zhao et al., 2016), TiO_2 (He et al., 2016), Al_2O_3 (Cimino and Scala, 2016) have been widely used in the process of flue gas mercury removal due to high specific surface area and mechanical strength, resulting in that the active components were easily coated onto the supporter surface. The modification of adsorption material can significantly improve the ability of mercury removal, which is an effective mean to control mercury emission in flue gas.

With the increase of CO emissions, the use of catalytic oxidation method to remove CO in flue gas has gradually become a hot research topic, and the heat released by catalytic combustion of CO is beneficial to the subsequent treatment of flue gas. Noble metal catalysts are considered to be an effective means for catalytic oxidation of CO, as reported by Zhang et al. (2017b), the nano-composite of Ag/Pr_6O_{11}-NRs (nano-rods) demonstrated a higher catalytic activity for CO oxidation with about 98.7% conversion at 210 °C, which might be ascribed to the meso-porous features, resultant oxygen vacancies of nano-rods support, as well as the large surface area and homogeneous loading of Ag species. Zhang et al. (2016b) found that Ag/HMS-450 (hexagonal mesoporous silica) can removal 50% CO at 50 °C and exhibited lower-temperature of catalytic activity (98% CO conversion at $T_{98\%}$=105 °C). However, the high economic burden for the preparation cost of noble metals is critical to the application for CO oxidation of one of the constraints. Zhang et al. (2016a) reported that CeO_2 alone has any activity at the temperature below 200 °C, while MnOx-CeO_2 catalyst has an excellent redox property for CO oxidation followed the Mars-van Krevelen (MK) mechanism ($T_{10\%}$=66 °C, $T_{100\%}$=190 °C) due to the incorporation of Mn^{n+} into the CeO_2 lattice resulting in two redox couples of $Mn^{4+}\rightarrow Mn^{3+}\rightarrow Mn^{2+}$ and $Ce^{4+}\rightarrow Ce^{3+}$. CuO/cryptomelane catalyst constituted by copper and manganese oxides showed the best performance when tested under $CO+H_2+O_2$ mixture, reaching its maximum CO conversion of 95% at 125 °C and keeping after that temperature a stable conversion of 88% (Davó-Quiñonero et al., 2017). Manganese oxide doped by Cu (Song et al., 2017), Co (Liu et al., 2017a) and Ce (Arena et al., 2017; Zhang et al., 2017a) could have a good CO catalytic activity in a wide temperature range.

Currently, to our knowledge, there is no reported research on the simultaneous removal of elemental mercury and CO in flue gas. As we known, carbon materials including active carbon and active coke etc. have been widely utilized in air purification and separation due to their large number of well-distributed micro-pores, high adsorption speed and high surface area. Carbon materials have been widely utilized in air purification and separation due to its large number of well-distributed micro-pores, high adsorption speed and high surface area. In recent years, activated coke (AC) has been successfully applied as the commercial material to the industrial desulfurization. Thus, in this work, catalytic materials were prepared using activated coke as supporter and transition metal oxide (Co, Cu, Ce, Mn, Fe) as active components. The loading and calcination conditions for optimizing the Cu and Co modified AC were further investigated to enhance the synergic-removal ability of CO and Hg^0 over the catalytic materials. The synergistic catalytic mechanism was also proposed on the surface of optimal Cu-CoOx/AC. This work provides a certain reference value for preparing catalytic materials to obtain the simultaneous removal of CO and Hg^0 with high efficiency at low temperature.

1. Experimental details

1.1. *Catalysts preparation*

Active coke (AC) as the supporter was purchased from Beishankou Zhuqing Activated Carbon Factory (Gongyi city in China, https://gyzq999.1688.com). The AC particles sieved into 40–60 mesh size were pretreated with 4 wt.% HNO_3 in water bath at 75 °C for 3 hr and then washed with ultrapure water until the pH had no change and dried in oven at 110 °C for 8 hr, which were named as AC_N. AC_N supported metal oxide catalysts (MOx/AC_N, M = Co, Cu, Ce, Mn or Fe) were prepared by an ultrasonic-assisted equivalent-volume impregnation method with the corresponding metal nitrate as precursor. The mass loading content was investigated as 10 wt.% for the single metal oxide. The materials were dried and calcined at a designed temperature for 4 hr in a muffle furnace with N_2 atmosphere. The best ones of above catalysts were further prepared with different mass loading and defined as y% MOx/AC_N, in which M stands for the loaded metal, and y (y = 2, 4, 6, 8, 10 and 12) for the load value from mass ratio of M to AC_N. Such as 10%$CoOx/AC_N$ sample was optimized for CO catalytic oxidation. Then, the optimal catalysts were further modified as z%CuO-10%$CoOx/AC_N$ (z = 2, 4, 6, 8, and 10) through step-

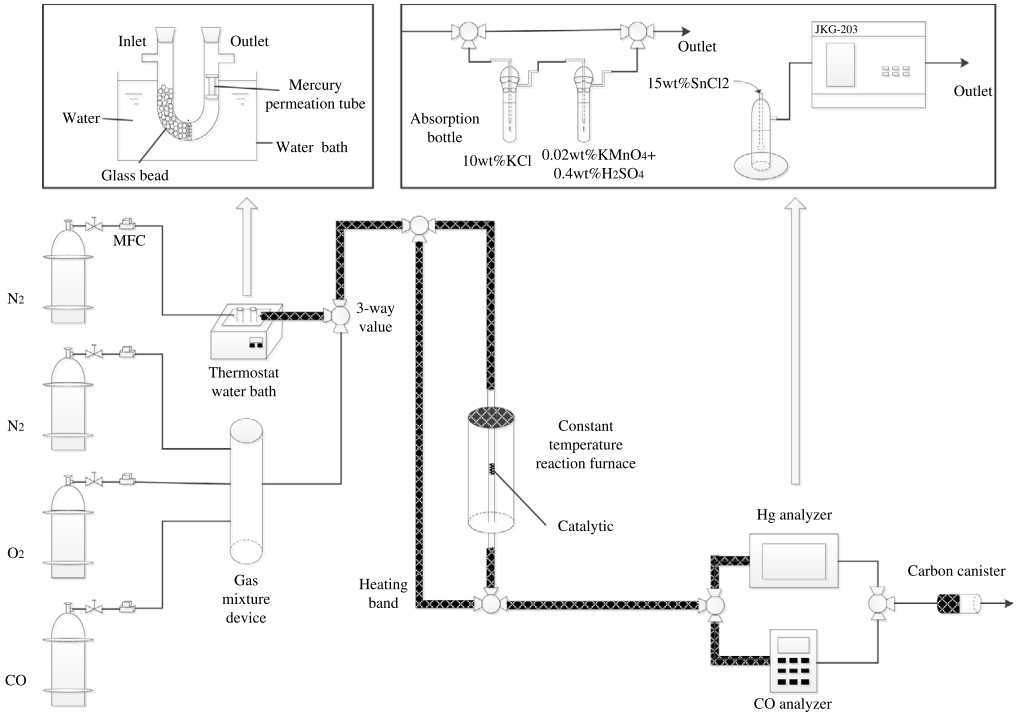

Fig. 1 – Schematic diagram of experimental setup.

by-step impregnation process for the simultaneous catalytic oxidation of CO and Hg^0.

1.2. *Characterization of samples*

Brunauer-Emmett-Teller (BET) method was adopted to clear the specific surface area of different samples, which was tested on Quadrasorb SI analyzer via N_2 adsorption. Microstructures including pore volume and size were analyzed by Horvath-Kawazoe method. The speciation of Co and Cu elements on the surface of different samples were analyzed by XRD method, which was tested by TTRIII multifunctional X-ray diffraction with Co kα radiation (2θ range of 5–90°). Scanning Electron microscope (SEM) was observed by using the Hitachi SU 8000 SEM, and an energy-dispersive X-ray spectrometer (EDS) was used to examine the distribution of the elements on the surface. Thermogravimetric analysis (TGA) was obtained on a Mettler TGA/DSC 1 SF/1382 system from 25 to 700 °C with 10 °C/min in the pure N_2 gas atmosphere.

The reduction characteristics of catalysts were analyzed by H_2-TPR profiles using a chemisorption analyzer with 100 mg of the sample and 5 vol.% H_2 in N_2 during the TPR process. Cold trap was used to avoid the disturbance of overflowing H_2O on the TPR signal. The valence changes of active elements over the surface of fresh and used catalysts were analyzed by XPS method, which was corrected by C1s binding energy at 284.6 eV.

1.3. *Experimental section*

The catalytic performances of the catalysts above for CO oxidation and Hg^0 oxidation removal were evaluated at a dynamic reaction system, which contains the units of gas supply, Hg^0 generator, gas mixer, reactor with temperature controller, and gas detector, as shown in Fig. 1. Hg^0 was obtained by a permeation tube of mercury (VICI Metronics of USA) with N_2 stripping after the mixed gas below, which could produce a certain weight of Hg^0 at designed temperature. Other gas components were derived from the corresponding cylinder gases, and then mixed equably in the blending tank. The total gas flow was set as 300 ml/min, equating to a gas hourly space velocity (GHSV) of 56,600 h^{-1}. The simulated flue gas was constituted by 50 μg/m^3 Hg^0, 10vol.% O_2, 5000 ppm CO, and N_2 balance.

Flue gas analyzer (KM 9106, UK) was used to detect the concentration of CO and O_2 from the inlet and outlet of reactor. Cold atomic mercury analyzer (JKG-203, China) was used to detect the concentration of Hg species as the following step: the airflow was accessed into impinge with absorption solution (10%KCl or 0.4%H_2SO_4+0.02wt.% $KMnO_4$), then the conversion from Hg^{2+} to Hg^0 could happen append of 15wt.% $SnCl_2$ before the analyzer. Finally, the airflow was accessed into the carbon trap to avoid toxic components discharged into atmosphere.

1.4. *Evaluation of catalytic activity*

The Hg^{2+} and Hg^0 were captured by the absorption solution of 10%KCl and 0.4%H_2SO_4+ 0.02 wt.%$KMnO_4$, the data was detected and calculated by cold atomic mercury analyzer was remembered as $C_{(Hg}2+)$ and $C_{(Hg}0)$.

About 0.1 g catalysts was used for each test. The reaction time of test was continued 6 hr. The detection of inlet and outlet of simulated flue gas was carried on at every 1 hr. In this

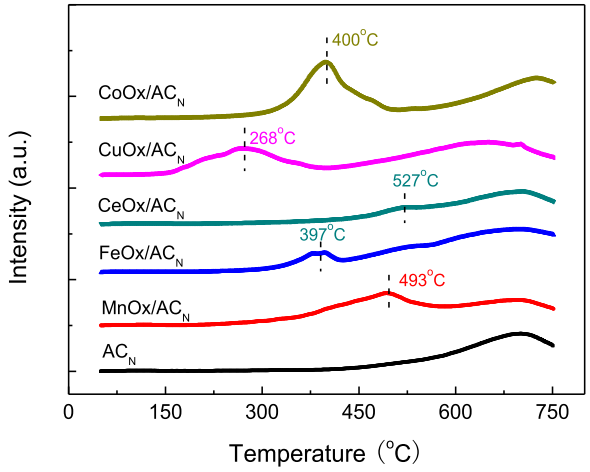

Fig. 2 – H_2-TPR profiles of various AC_N supported metal oxides.

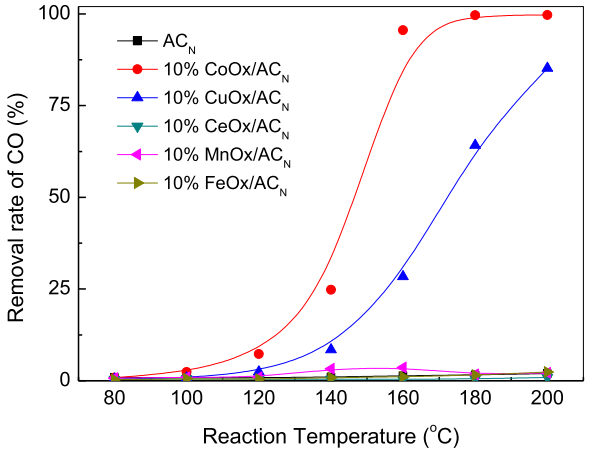

Fig. 3 – CO oxidation efficiency over series of MOx/AC_N catalysts (M=Cu, Ce, Co, Fe, Mn) for the individual catalysis. Reaction conditions: gas flow of 300 ml/min, GHSV = 56,600 h^{-1}, [CO] = 5000 ppm, [O_2] = 10vol.%, and N_2 balance.

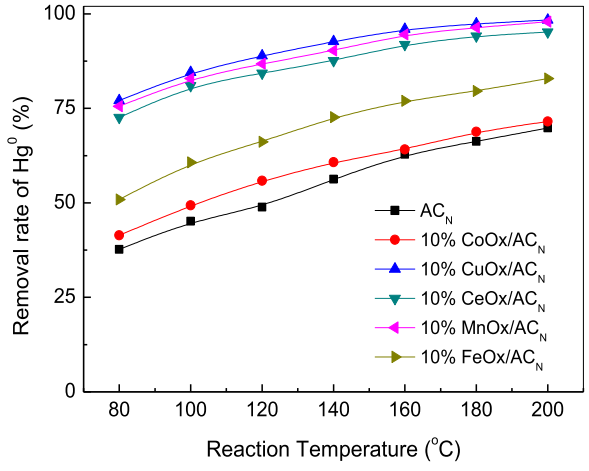

Fig. 4 – Hg^0 removal efficiency over series of MOx/AC_N catalysts (M = Cu, Ce, Co, Fe, Mn) for the individual catalysis Reaction conditions: gas flow of 300 ml/min, GHSV = 56,600 h^{-1}, [Hg^0] = 50 μg/m^3, [O_2] = 10 vol.%, and N_2 balance.

work, the removal rate of Hg^0 in simulated flue gas was calculated by the following Eq. (1), and the penetration rate of Hg^{2+} in simulated flue gas was calculated by following Eq. (2).

$$\eta_{(Hg^0)} = \frac{C^0_{Hg^0} - \left[C_{Hg^0} + C_{Hg^{2+}}\right]}{C^0_{Hg^0}} \times 100 \quad \text{(Eq.1)}$$

$$\eta_{(Hg^{2+})} = \frac{C_{Hg^{2+}}}{C^0_{Hg^0}} \times 100 \quad \text{(Eq.2)}$$

Here, $C^0{}_{(Hg^0)}$ is the concentration of Hg^0 of inlet simulated flue gas, $C_{(Hg^{2+})}$ and $C_{(Hg^0)}$ is the concentration of $Hg^{2+}$and Hg^0 of outlet simulated flue gas. Only negligible amounts of Hg^{2+} were detected.

Meanwhile, the removal rate of CO in simulated flue gas was calculated by the following Eq. (3).

$$\eta_{(CO)} = \frac{C^0_{CO} - C_{CO}}{C^0_{CO}} \times 100 \quad \text{(Eq.3)}$$

Here, $C^0{}_{(CO)}$ and $C_{(CO)}$ stands for the CO concentration of inlet and outlet simulated flue gas, respectively.

2. Results and discussion

2.1. *Separate catalytic oxidation of CO, Hg^0*

2.1.1. *Search for active component*

The H_2-TPR profiles of various MOx/AC_N catalysts (M = Cu, Ce, Co, Fe, Mn) were obtained to define the oxides form and analyze the redox capacity. As shown in Fig. 2, the reduction peak at the temperature higher than 600 °C was found on each catalysts because of the self-decomposition of carbon material (as shown in following TGA section in Fig. 9) (Yi et al., 2018), which were suppressed to a certain extents after modifying by active components. For the modified catalysts, peak at 493 °C over $MnOx/AC_N$ was detected as the transformation of $Mn_3O_4 \rightarrow MnO$ (Zhang et al., 2011), peak at 397 °C for $Fe_2O_3 \rightarrow FeO$ over $FeOx/AC_N$ (Zhang et al., 2018), peak at 527 °C for $CeO_2 \rightarrow CeO$ over $CeOx/AC_N$ (Chen et al., 2016), peak at 268 °C for $CuO \rightarrow Cu_2O$ over $CuOx/AC_N$ (Wang et al., 2018), and peak at 400 °C for $Co_3O_4 \rightarrow CoO$ over $CoOx/AC_N$ (Chen et al., 2016), respectively. It should be pointed out that $CoOx/AC_N$ and $CuOx/AC_N$ samples presented the higher hydrogen consumption peak at the relative low temperature, indicating that these two catalysts might have strong redox ability being favorable for catalytic reaction.

The individual catalytic oxidation of CO and catalytic removal of Hg^0 over the above catalysts were performed separately, and the catalytic activities are given in Figs. 3 and 4, respectively. In Fig. 3, it can be seen clearly that $CeOx/AC_N$, $FeOx/AC_N$ and $MnOx/AC_N$ hardly had the catalytic activity

for CO oxidation at the designed temperature range of 80–200 °C, while the CO oxidation efficiency of CoOx/AC_N and CuOx/AC_N were both increased as the reaction temperature increasing. CoOx/AC_N catalyst obtained the CO oxidation efficiency of 95–100% at temperature above 160 °C, which was obviously superior to CuOx/AC_N with its highest activity of 85.2% at 200 °C. It might be contributed to the excellent oxidation performances of CoOx/AC_N and CuOx/AC_N for the good catalysis activity of CO oxidation, which was evidenced by the H_2-TPR results. It has been proven that Co_3O_4 has high catalytic activity in CO oxidation reaction (Jansson et al., 2002; Wang et al., 2007). Zhang et al. (2012) found that bulk Co_3O_4 presented risen activity for CO oxidation of ~64% at 120 °C and >97% at 140 °C, and expected that the low-temperature activity was mainly correlated with the electronic migration between Co^{3+} and Co^{2+}. CuOx and Cu-containing catalysts with the mixture phases of CuO and Cu_2O presented more active for CO oxidation (Gu et al., 2014; Penkala et al., 2018), benefiting from that the Cu-phase became amorphous during reduction and followed by re-oxidation under the oxidizing atmosphere (Penkala et al., 2018).

It has been reported that the CeO_2 alone has an inferior activity because of the slow release of oxygen without other cations (Stošić et al., 2012), while the doping of other cations into CeO_2 lattice generating to Ce-based solid solutions was proven superior catalytic activity to the metal oxide alone, which was probably owned to doping generated defects or new mixed oxide phases (Collins et al., 2010). Xu et al. (2014) found that MnOx presented the oxidation of CO might proceed through the Langmuir-Hinshelwood (LH) mechanism being responsible from the adsorbed oxygen (< 200 °C) to the Mars-van Krevelen mechanism with increasing reaction temperature. Ramesh et al. (2008) has reported an activity order of CO oxidation as: MnO < MnO_2 < Mn_2O_3 below 250 °C, in which LH mechanism was performed for the catalytic oxidation of CO over Mn_2O_3 and MnO_2 catalysts, and MK mechanism for MnO sample. However, the CO oxidation activity of MnOx was remarkably influenced by the crystal phase (Mn^{2+}-Mn^{7+}) with different Mn-O bond strength and its mixtures with the second/other metal oxide (Zhang et al., 2016a). Based on above analysis, it was not hard to understand that the ultra-low catalytic activity for CO oxidation over simple CeOx/AC_N and MnOx/AC_N might mainly due to the unsustainable redox couple without other cations in our studies.

From Fig. 4, all the designed metals to modify the AC_N could improve the removal capability of Hg^0 with the increase of reaction temperature. The removal ability of Hg^0 oxidation over the different metal doped AC_N could be sorted as follows: Cu > Mn > Ce >>>Fe >> Co > None. CuOx/AC_N catalyst obtained the removal efficiency of above 96% when the reaction temperature was higher than 160 °C, while MnOx/AC_N and CeOx/AC_N had less activities within the gap of 5% at each temperature points. In contrast, the promoting effects of FeOx and CoOx on Hg^0 removal were greatly inferior to the above three catalysts, especially that CoOx/AC_N showed an even weaker increase than the virgin AC_N catalyst. Xu et al. (2014) found that the order of different active components supported on TiO_2 for Hg^0 removal was as follows: CuO > Fe_3O_4 > MnO_2 > CeO_2 > Co_3O_4. Cu ion has a more effective nuclear charge and a type of unfilled orbital structure, which makes CuO perform best in the removal of Hg^0.

2.1.2. *Optimization of Co_3O_4 or CuO loads*

It has been confirmed from the results in Fig. 3 and Fig. 4 that Co and Cu has reactivity for the catalytic oxidation of CO and the removal of Hg^0, respectively. It was one of the important factors for reactivity that loading different amount of Co or Cu, and series of *x*%CoOx/AC_N and *y*%CuOx/AC_N catalysts (*x or y* = 2, 4, 6, 8, 10, 12) were prepared and used to obtain the optimum loading amount (10% for CoOx and 8% for CuOx) at the designed loading ranges, as shown in Fig. 5. For the catalytic oxidation of CO, the samples of 2%CoOx/AC_N and 2%CuOx/AC_N had hardly any oxidation efficiency. However, the CO oxidation efficiency were enhanced obviously as the increase of loading amount within the optimum load and also reaction temperature. It indicated that transition metal loading of Co or Cu improved the catalytic oxidation reactivity of CO, but further increasing the load might cause the decrease of specific surface area that resulting in the decrease of catalytic activity. The CO oxidation efficiency of 8%CuOx/AC_N was 91.2% at 200 °C, which was significantly lower than that of 95% at 160 °C and 99.7% at 200 °C over 10%CoOx/AC_N. It indicated that Co doping was more effective to improve the reactivity than Cu doping. Zhao et al. (2014) considered that Co_3O_4 was more excellent performance than CuO catalyst for CO oxidation at wider range of temperature. For the oxidation removal of Hg^0, the promotion effect over AC_N was lower by loading of Co-species, and it was about 1.3%–6.7%-up by optimum loading amount. The Hg^0 removal efficiency was promoted from 37.7%–69.8% to 50.1–86.4% by loading of 2%CuOx, and 8%CuOx/AC_N made this value to 79.1%–98.9% at the designed temperature range, respectively. In our previous study (Zhao et al., 2016), it also has been confirmed that 8% load was optimum loading amount of CuO for Hg^0 removal. The oxidation removal of Hg^0 was great promoted by loading of Cu, and the catalytic oxidation of CO was great promoted by loading of Co, indicating that the active sites were different for the oxidation of Hg^0 and CO. Thus, the catalytic materials for simultaneous removal Hg^0 and CO could be prepared by loading of Cu and Co.

2.2. *Simultaneous removal of CO and Hg^0 over Cu-CoOx/AC_N catalysts*

2.2.1. *Effect of Cu load*

It has been found that 10% CoOx/AC_N presented the best activity for CO oxidation as given above. In this section, a series of *z*% CuOx-10% CoOx/AC_N catalysts (*z* = 0, 2, 4, 6, 8, 10) were prepared for the simultaneous catalytic oxidation of CO and Hg^0. The CO oxidation efficiency and the Hg^0 removal efficiency are given in Fig. 6, which was carried out at 180 °C. It is clear that, among the bimetallic oxides with different mass ratio, 2%CuOx–10%CoOx/AC_N catalyst has high activity for the synchronous catalysis of CO oxidation (69.7%) and Hg^0 removal (73.2%). It should be clarified that this sample presented the obvious decrease of CO oxidation efficiency compared with Co_3O_4/AC_N (~100%), and displayed little lower Hg^0 removal efficiency (10%Co_3O_4/AC_N, ~65%), suggesting that the

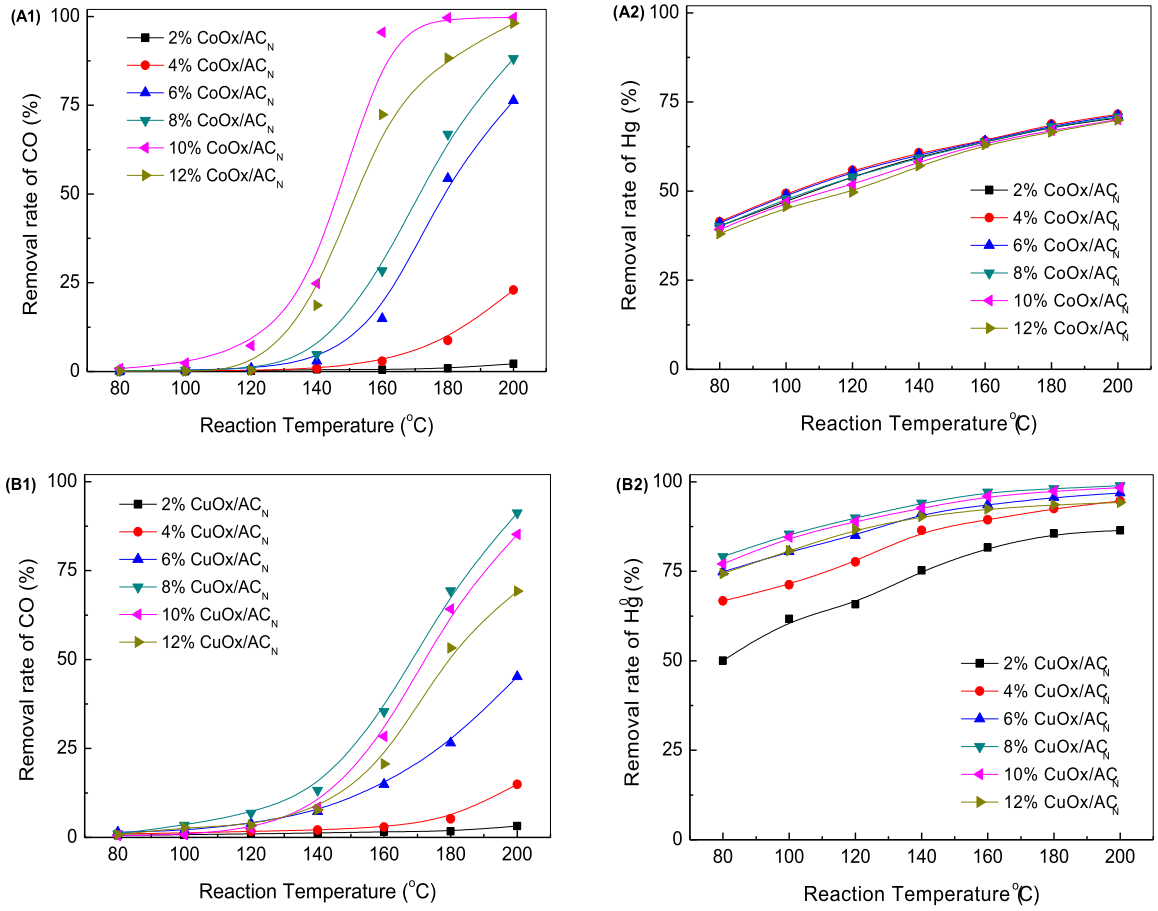

Fig. 5 – CO oxidation efficiency (A1, B1) and Hg^0 removal efficiency (A2, B2) over various $CoOx/AC_N$ (A1, A2) and $CuOx/AC_N$ (B1, B2) catalysts with different load for the individual catalysis. Reaction conditions: gas flow of 300 ml/min, GHSV = 56,600 h^{-1}, [CO] = 5000 ppm or [Hg^0] = 50 μg/m^3 when used, [O_2] = 10 vol.%, and N_2 balance.

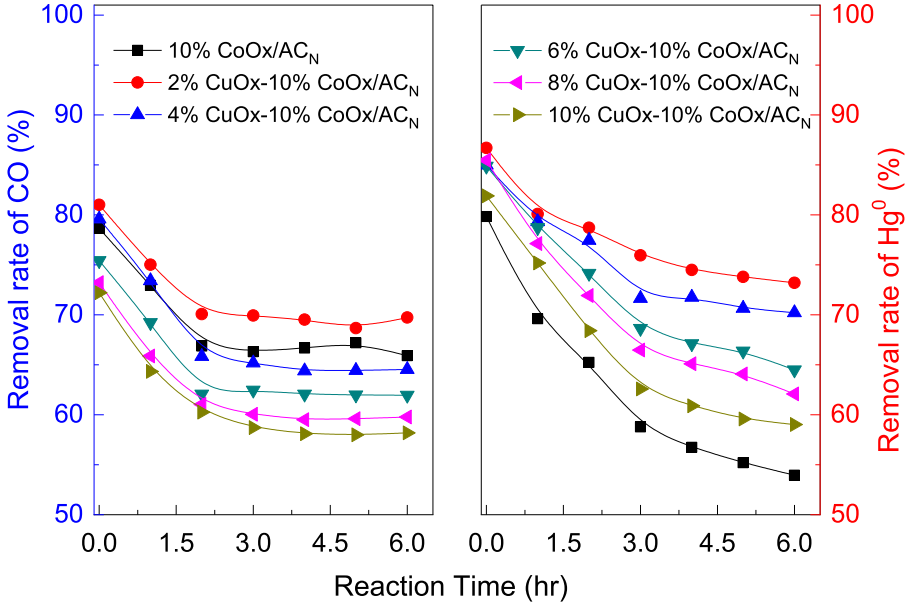

Fig. 6 – CO oxidation and Hg^0 removal efficiency over various z%CuOx-10%$CoOx/AC_N$ catalysts with different Cu load for the simultaneous removal of CO and Hg^0. Reaction conditions: gas flow of 300 ml/min, GHSV = 56,600 h^{-1}, [CO] = 5000 ppm and [Hg^0] = 50 μg/m^3, [O_2] = 10 vol.%, and N_2 balance, reaction temperature at 180 °C.

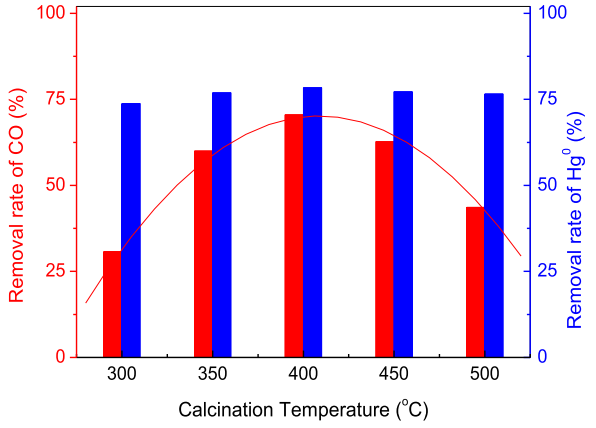

Fig. 7 – CO oxidation efficiency and Hg^0 removal efficiency over various 2%CuOx-10%CoOx/AC_N prepared at different calcination temperature. Reaction conditions: gas flow of 300 mL/min, GHSV = 56,600 h^{-1}, [CO] = 5000 ppm and [Hg^0] = 50 μg/m^3, [O_2] = 10 vol.%, and N_2 balance, reaction temperature at 180 °C.

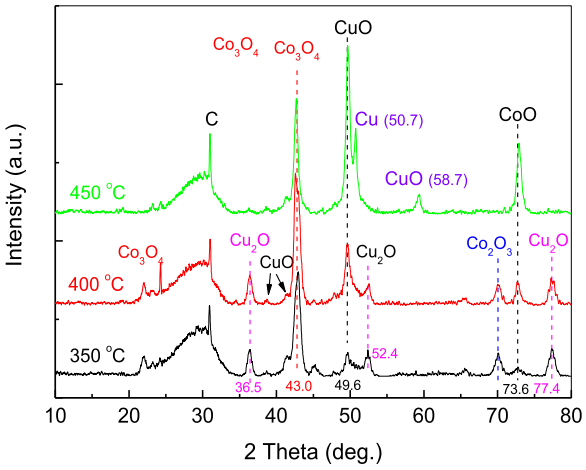

Fig. 8 – XRD patterns of 2%CuO-10%Co_3O_4/AC_N prepared at 350, 400 and 450 °C.

introduction of Hg^0 has a negative influence on the oxidation of gaseous CO while the CO has weak effect on Hg^0 removal. This phenomenon might be due to the following reasons: (1) A part of Co-sites were covered by CuOx species resulting in the decrease of the CoOx active components for CO oxidation, as we found that in Fig. 5(A1), 8% CoOx/AC_N sample gave a low-down CO oxidation efficiency than 10%CoOx/AC_N while 2%CuOx/AC_N has negligible activity; (2) Although CuOx species has apparent activity for Hg^0 removal (negligible Co-sites), the mass loading content was just of 2 wt.% which provided limited sites but effective for the removal of Hg^0. It was a negative factor for CO oxidation efficiency as the load amount of Cu was increasing above 2%, resulting in the lower activity as load increasing than that of the fresh Co_3O_4/AC_N catalyst. Although more Cu load (>2%) leaded to the decrease of Hg^0 removal efficiency, it revealed better activity than that of virgin Co_3O_4/AC_N catalyst. In general, the catalytic activity might be affected by the special surface area and pore structure of catalysts (Zhao et al., 2016; Zhao et al., 2019). BET surface area of 10%Co_3O_4/AC_N, 2%CuOx-10%CoOx/AC_N, and 4%CuOx-10%CoOx/AC_N were obtained, in which 2%CuOx-10%CoOx/AC_N showed a little decrease within 1.6% of surface area than 10%Co_3O_4/AC_N (425.6 m^2/g) but a significant increase in microspore area to 365.7 m^2/g (from 83.8% to 87.3%), while 4%CuOx–10%CoOx/AC_N presented a significant reduction of BET surface area to 381.8 m^2/g (-10.3%). This might be one important reason for facilitating the simultaneous oxidation of CO and Hg^0 over 2%CuOx-10%CoOx/AC_N catalyst.

2.2.2. *Effect of calcination temperature*

The effects of calcination temperature on the simultaneous catalytic oxidation of CO and Hg^0 were performed, as shown in Fig. 7, which was obtained at 180 °C and run for 3 hr (due to the nearly balanced points from Fig. 6). It was found that calcination temperature has a very little impact on the oxidation efficiency of Hg^0 within the gap of 4.7% compared to the best of 78.4% over 2%CuOx–10%CoOx/AC_N calcinated at 400 °C, which was might due to that the mixture copper oxide species (Cu^{2+} and Cu^+) were both active for reaction during reduction and followed by re-oxidation (Penkala et al., 2018). While for CO oxidation, the 2%CuOx–10%CoOx/AC_N catalyst presented a parabolic trend with the best activity of 70.5% centered at 400 °C during increasing the calcination temperature from 300 to 500 °C. The catalyst prepared at 300 °C has the lowest CO oxidation efficiency of about 30.8%, and 2%CuOx–10%CoOx/AC_N (500 °C) showed a slightly better activity to 43.6%. This results indicated that calcination temperature greatly affects the existent form and valence state of CoOx with different redox properties during calcinating at different temperature, resulting in the significant difference efficiencies for CO oxidation.

XRD characterizations were carried out to receive the crystal structure information of catalyst material calcined at 350, 400 and 450 °C, respectively. As shown in Fig. 8, the characteristic peaks of metal nitrate could not be found, which indicated that the precursors could be decomposed completely at those temperatures. The phases were composed by CuO, Cu_2O, Co_3O_4 and Co_2O_3 when calcination temperature was 350 °C, while the phase was composed by CuO, Cu_2O, Co_3O_4, Co_2O_3 and CoO when calcination temperature was 400 °C, and furthermore the phase was composed by CuO, Cu, Co_3O_4 and CoO when calcination temperature was 450°C. It meant the change of CuO→Cu_2O→Cu and Co_2O_3→Co_3O_4→CoO was happened with rising the calcination temperature (Zhao et al., 2016). The peak strength of Cu-species (CuO, Cu_2O and Cu) was weaker than the Co-species (Co_3O_4, Co_2O_3 and CoO), which was attributable to the loading amount of copper was lower than cobalt. The main phase of Co-species was Co_3O_4 when calcination temperature was 400 °C (the optimal value), which indicated that Co_3O_4 (configuration of Co_2O_3 and CoO) might was an important role in the removal of CO oxidation. For Cu-species, the main phase was not clear, which was attributable to Cu_2O was easily produced on AC when Cu doped AC was calcined at 400 °C (Zuo et al., 2015). The coexistence of complex oxides including CuO and Cu_2O, Co_3O_4 and Co_2O_3 would likely be beneficial to the simultaneous catalytic oxidation of

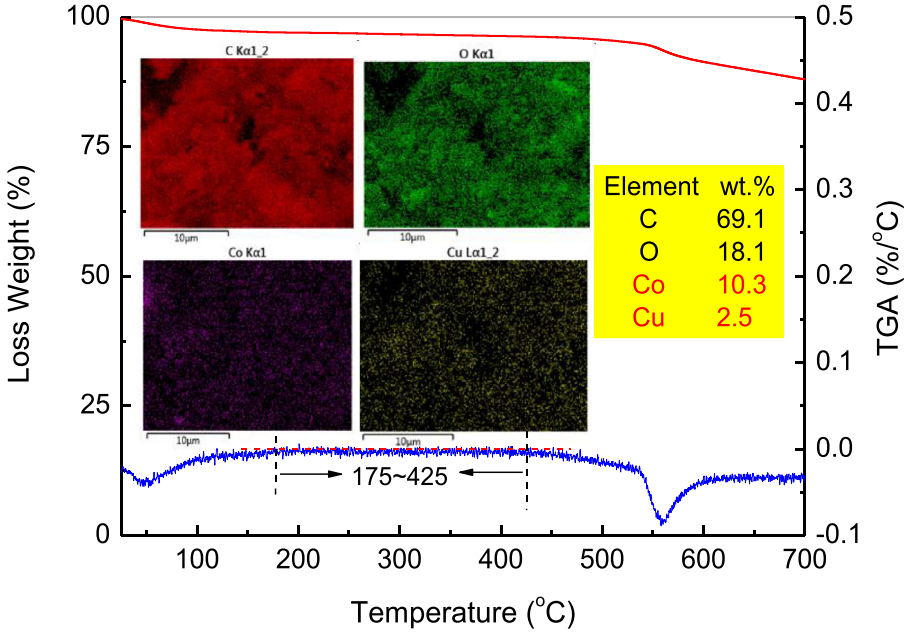

Fig. 9 – Thermodynamic stability and element distribution (illustration) of 2%CuOx-10%CoOx/AC$_N$ (400°C).

CO and Hg^0 over Cu-CoOx/AC$_N$ catalysts, which will be evidenced by the XPS analysis motioned below.

Fig. 9 shows the thermodynamic stability in the pure N_2 gas atmosphere of Cu-CoOx/AC$_N$ catalyst prepared at 400 °C, which presented a stable performance at the temperature range of 175–425 °C. In the figure, the peaks at lower temperature and centered at 560 °C might be ascribed to the release of H_2O and COx-species of active coke, respectively. In the illustration in Fig. 9, it could make clear that the Co- and Cu-species were successfully loaded and gave a relatively uniform distribution onto the catalyst surface. The loads of Co- and Cu- was 10.3 wt.% and 2.5 wt.%, respectively, which was in close proximity to the theoretical designed value. This result explained that the Cu-CoOx/AC$_N$ catalysts were successfully prepared using the designed method and met the expected aim.

2.2.3. *Effect of reaction temperature*

Fig. 10 gives the simultaneous removal efficiency of CO and Hg^0 as a function of reaction temperature over 2%CuOx–10%CoOx/AC$_N$ catalyst calcinated at 400°C (noted as Cu-CoOx/AC$_N$ in the following sections). It can be found that the catalysis removal of CO oxidation on Cu-CoOx/AC$_N$ catalyst were obviously depended on the reaction temperature, which obtained 58.1% CO conversion at 160 °C, and 70.5% at 180 °C, and significantly increased to 94.7% at 200 °C. For the removal of Hg^0, there was no obvious promoting effect on catalytic activity of 68.3% at 140 °C to 76.7% at 200 °C, in which the best removal rate of Hg^0 was about 78.7% at the reaction temperature of 180 °C. This phenomenon could be explained that the adsorption and catalysis were existence/combination for the oxidation and removal of Hg^0, as proposed in our previous study over CuO/AC catalyst (Zhao et al., 2016), in which the increase of temperature would weaken Van-der-Waals forces for adsorption process while more kinetic energy was continually needed for chemical reaction progress. As a result, with the reaction temperature continually rising, the decrease of adsorption began to be a crucial factor when temperature was over 180 °C and thus maintaining the reaction balance of Hg^0 removal during the combination of adsorption and catalysis process (Xie et al., 2015).

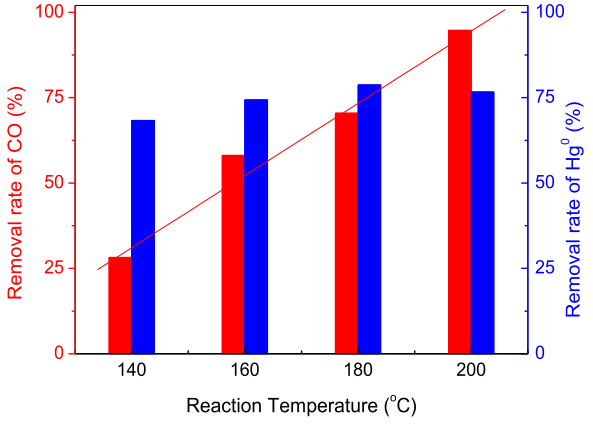

Fig. 10 – CO oxidation and Hg^0 removal efficiency as a function of reaction temperature over 2%CuOx-10%CoOx/AC$_N$ (400 °C). Reaction conditions: gas flow of 300 ml/min, GHSV = 56,600 h^{-1}, [CO] = 5000 ppm and [Hg^0] = 50 μg/m^3, [O_2] = 10 vol.%, and N_2 balance.

2.2.4. *Effect of oxygen content*

The effects of oxygen content on the simultaneous removal efficiency of CO and Hg^0 were presented in Fig. 11. 2%CuOx–10%CoOx/AC$_N$ was mostly inactive in the catalytic oxidation of CO and Hg^0 without the introduction of oxygen, while the removal efficiency of CO and Hg^0 were both greatly enhanced

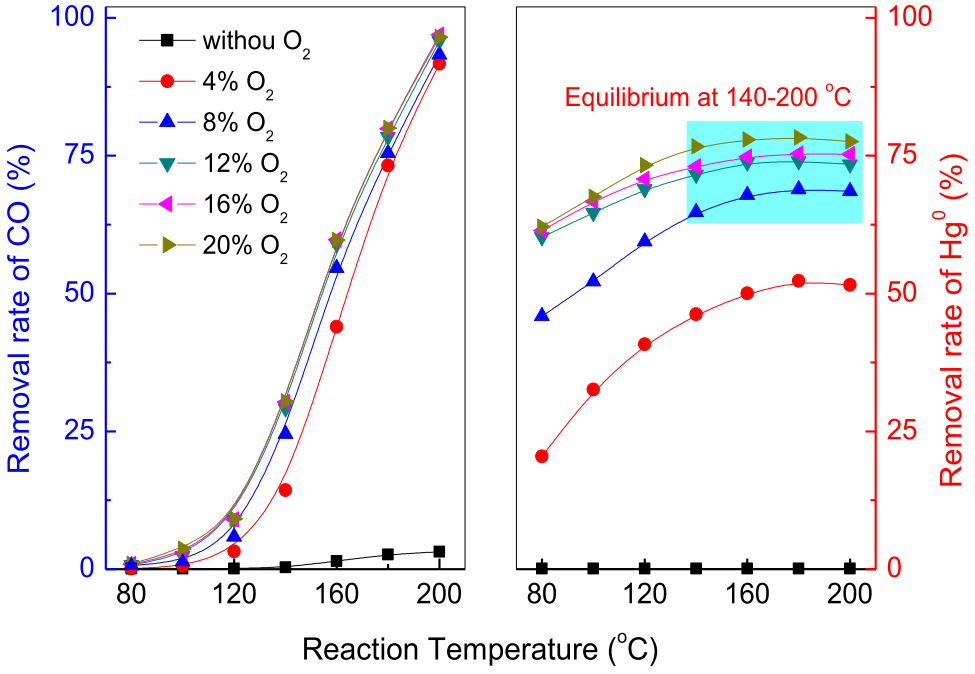

Fig. 11 – CO oxidation efficiency and Hg^0 removal efficiency as a function of oxygen content over 2%CuOx-10%CoOx/AC_N (400 °C). Reaction conditions: gas flow of 300 ml/min, GHSV = 56,600 h^{-1}, [CO] = 5000 ppm and [Hg^0] = 50 μg/m^3, [O_2] = designed contents, and N_2 balance.

as the oxygen content increasing to 4vol.%. The results indicated that oxygen was very importantly beneficial for the catalytic oxidation of CO and Hg^0. With the further increase of oxygen content, the CO oxidation activity showed a limited improvement while the removal rate of Hg^0 has a tremendous increase. As described above that the removal of Hg^0 was depended on the combined adsorption and catalysis, in which the adsorption processed continued to improve with the increase of O_2 in spite of balanced catalysis. In the case without O_2, it can be found that the CO oxidation efficiency was increased as the temperature raised above 160 °C, indicating lattice oxygen played the key roles in CO oxidation via the Mars-van Krevelen mechanism, in which the oxygen vacancies on the interface between metal cations were produced and further captured the gas-phase oxygen to form active interface oxygen species that could be easily extracted by CO to form CO_2 (Zhang et al., 2016a). Thus, it is a conviction that the more promoting effect was not obtained when the oxygen was enough for the catalytic oxidation of CO. It should be pointed out that Cu-CoOx/AC_N catalyst got the better CO oxidation activity and also high Hg^0 removal efficiency during the simultaneous catalysis with the oxygen content range of 8%–20%, which is very suitable for the multi-pollutants removal from flue gas with the conditions of high-concentration O_2 and gas temperature below 200 °C. We speculated that cheap binary oxides doped on activated coke will substitute for the removal of CO and Hg^0, especially operating under mild conditions.

2.2.5. *Simultaneous catalysis mechanisms of CO and Hg^0 over Cu-CoOx/AC_N*

In Fig. 12, the XPS spectra for O1s, Co2p, Cu2p and Hg4f of fresh and used Cu-CoOx/AC_N catalysts were performed to analyze the changes in surface species and relative content, and being beneficial to propose the simultaneous catalysis mechanisms of CO and Hg^0 over Cu-CoOx/AC_N. In Fig. 12(A), two distinguishing peaks at around 530.1 eV and 532-532.2 eV were exhibited, which was attributed to lattice oxygen (O_L) and surface adsorbed oxygen (O_S), respectively (Gao et al., 2019a; Gao et al., 2019b; Gao et al., 2020). The ratio of $O_S/(O_S+O_L)$ could reach high up to above 80% over both two samples, which might be benefited from the rich oxygenated functionality groups such as OH-/O_x-, CO-, and COO- species over carbon-based material promoting the adsorption of gases and catalytic redox process (Gao et al., 2018a). It was clearly found that the lattice oxygen of used sample was reduced significantly to 11.2% compared to 18.5% of the fresh one, indicating that the surface lattice oxygen involved in catalytic reactions directly to generate oxygen vacancies that would be replenished by gas-oxygen to generate the active oxygen species. Thus it was a evidenced that the relative concentration ratio of $O_S/(O_S+O_L)$ was increased to 88.8% from 81.5% after catalytic reaction, which implied that extra oxygen was absorbed in the course of reaction. The results given a good agreement with the co-existence of Langmuir-Hinshelwood (L-H) and Mars-van Krevelen (M-K) mechanism for CO catalytic oxidation and L-H mechanism for Hg^0 oxidation at low temperature. It should be noted that there was almost no Hg^{2+} leaved from gas stream out the reaction system, which implied that Hg^0 were oxidation to HgO or/and Hg^{2+} attached to the catalyst surface, as evidenced by the Hg4f XPS spectra (Fig. 12(D)) of used sample in which the peak at around 103.5 eV and 102.6 eV was divided into Hg^{2+} (generally HgO) and characteristic peak of Si2p over active coke, respectively (Chen et al., 2018b; Huang et al., 2016; Jampaiah et al., 2016). No peak of adsorbed

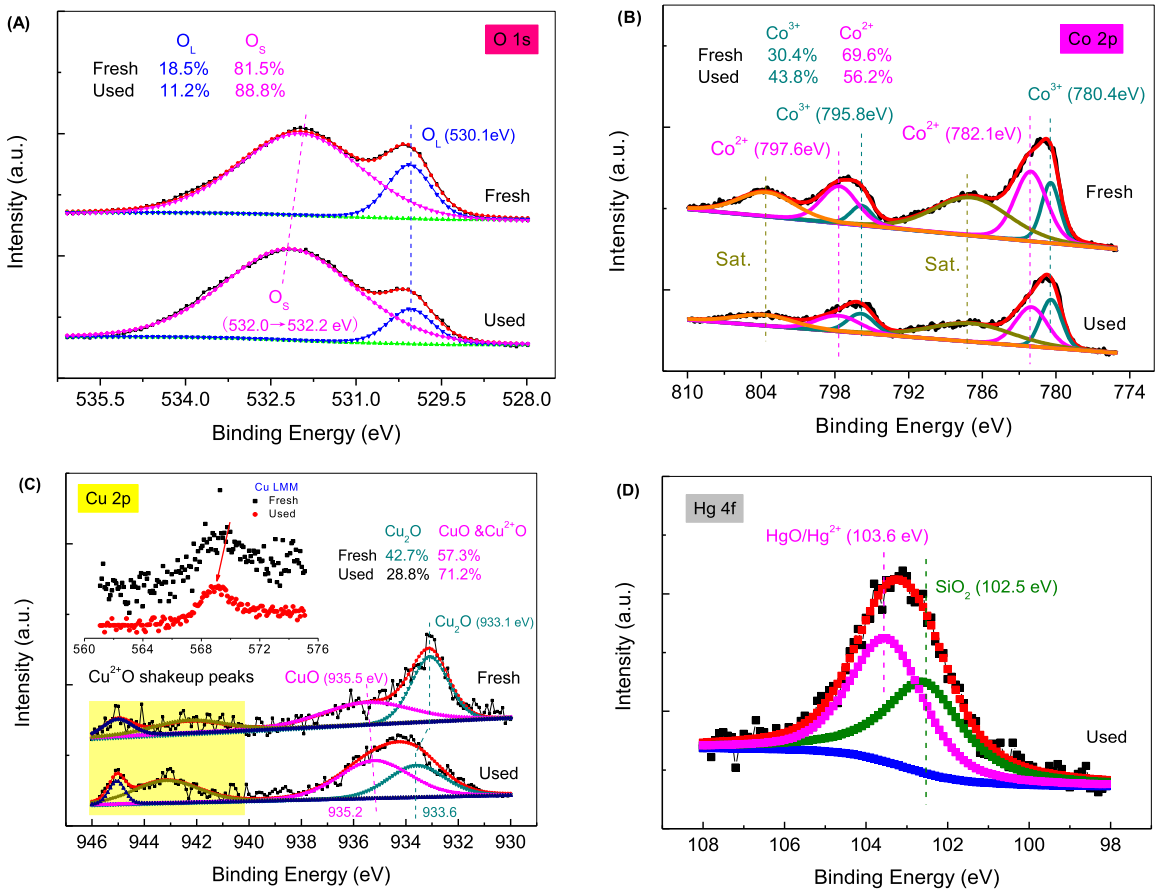

Fig. 12 – XPS spectra for O1s (A), Co2p (B), Cu2p and Cu LMM (C), and Hg4f (D) of fresh and used Cu-CoOx/AC$_N$ catalysts.

Hg^0 (at about 99.8 eV) was found on the surface of used catalysts.

It has been found that the Co- and Cu-species on the surface were in the form of mixed oxides according to the XRD results. Thus their phases were investigated by Co2p and Cu2p XPS spectra, as shown in Fig. 12(B) and (C), respectively. XPS spectra for Co2p were divided into six peaks attributed to Co^{3+} (780.4 eV, 795.8 eV), Co^{2+} (782.1 eV, 797.6 eV), and the satellites (786.9 eV, 803.6 eV) (Gao et al., 2018b; Meng et al., 2018; Tang et al., 2015). XPS spectra for Cu $2p_{3/2}$ were included into Cu_2O (933.1–933.6 eV) and CuO (935.2–935.5 eV, shakeup peaks) (Chen et al., 2018a; Liu et al., 2017b). No peak at around 567.8 eV was found for Cu° from Cu LMM spectra. It can be found obviously that the phases of Co^{3+} and Cu^{2+} were enhanced instead of the decrease of $Co^{2+}O$ and Cu_2O during the catalytic reactions for simultaneous oxidation of CO and Hg^0.

The experimental results had found that Co-species were the main active sites for CO oxidation and Cu-species for Hg^0 removal, and that the doping of 2%CuOx on 10%CoOx/AC$_N$ catalyst has an obvious promoting effect on both CO oxidation and Hg^0 removal. It might be benefiting from the synergistic catalysis during the electro-interaction between Co and Cu cations ($CoO \rightleftharpoons Co_3O_4$ and $Cu_2O \rightleftharpoons CuO$), which was coincided with the reports Gu et al., 2014; Xie et al., 2015; Zhang et al., 2016a). Meanwhile, the higher reactive activity was still being maintained after catalytic reaction of 6 hr, and Co- and Cu- species also showed a good catalytic activity for removal Hg^0 and CO, respectively, which implied that Co_3O_4 and CuO were active sites for removal CO and removal Hg^0, respectively (Jansson et al., 2002; Xiang et al., 2012). Zhang et al. (2016a) found that CO oxidation followed distinct reaction routes during different temperature range, in which CO could reacted with the surface lattice oxygen directly to generate oxygen vacancies (direct route) and reacted with the adjacent O from surface OH to generate HCOO* intermediate decomposing into CO_2 (formate route) at the temperature below 130 °C, and that the reaction gone through the carbonate route via the adsorbed CO at oxygen vacancies reacted with the surface lattice oxygen to generate carbonate species at the temperature above 130 °C. Thus, in this section, it is a conviction that different oxidation mechanisms mainly based on the carbonate route might occurred over Cu-CoOx/AC$_N$ catalyst through increasing the temperature from 140 to 200 °C, resulting in noticeable increase of CO oxidation activity. Based on the above analysis, we proposed that the removal of Hg^0 including Reactions ((1) to (6) followed the route R1 for adsorption process (gaseous Hg^0 species were adsorbed onto the surface of active coke and further oxidized to HgO/Hg^{2+} spices by surface active oxygen) and the route R2 for catalytic oxidation (gaseous Hg^0 species were adsorbed and oxidized to HgO/Hg^{2+} spices by CuO active sites during $Cu_2O \rightleftharpoons CuO$), and the catalysis of CO to CO_2 abided by the Mars–van Krevelen mechanism with lattice oxygen species including Reactions (7) to (12) via the reaction processes by the RI route (gaseous CO was directly

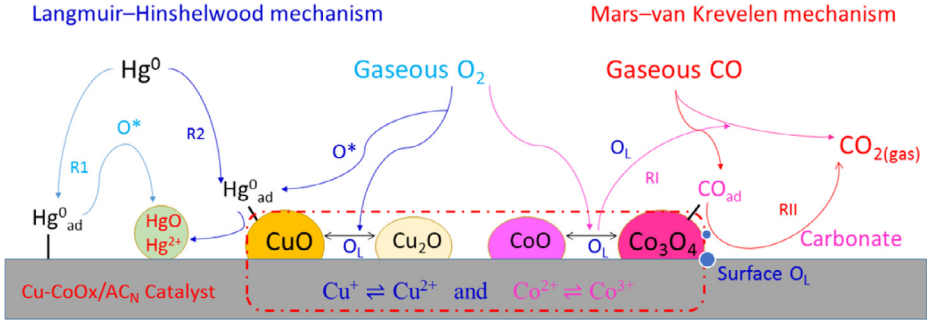

Scheme 1. – Proposed synergetic-catalysis mechanisms for the oxidation of gaseous CO and Hg^0 over Cu-CoOx/AC_N catalyst.

oxidized to CO_2 by lattice oxygen during CoO⇌Co_3O_4) and the RII route (CO was adsorbed onto the Co_3O_4 surface and further oxidized to carbonate spices by surface active oxygen, finally the intermediate spices were decomposed into gaseous CO_2), as presented in Scheme 1.

$$O_{2(gas)} + * \rightarrow O* + O* \quad (1)$$

$$O_{2(gas)} \xrightarrow{\text{vacancoes}} [O_L] + [O_L] \quad (2)$$

$$Cu_2O + [O_L] \xrightarrow{-e} 2CuO \quad (3)$$

$$Hg^0_{(gas)} \rightarrow Hg^0_{(ads)} \xrightarrow{[O*]} HgO_{(ads)} \quad (4)$$

$$Hg^0_{(ads)} + O* \xrightarrow{CuO} HgO_{(ads)} \quad (5)$$

$$2CuO \xrightarrow{+e} Cu_2O + O* \quad (6)$$

$$CO_{(gas)} + [O_L] \xrightarrow{\text{vacancies}} CO_{2(gas)} \quad (7)$$

$$3CoO + O* \xrightarrow{-e} Co_3O_4 \quad (8)$$

$$CO_{(gas)} \xrightarrow{Co_3O_4} CO_{(ads)} \xrightarrow{O_L} -COx_{(ads)} \quad (9)$$

$$-COx_{(ads)} \xrightarrow{\text{decomposition}} CO_{2(gas)} + O* \quad (10)$$

$$Co_3O_4 \xrightarrow{+e} 3CoO + O* \quad (11)$$

$$O* + O* \rightarrow O_{2(gas)} \quad (12)$$

3. Conclusions

In this work, various MOx/AC_N catalysts (M = Co, Cu, Ce, Mn, Fe) were prepared for the separate catalytic oxidation of CO and Hg^0, in which Co has good catalytic activity of CO oxidation, and Cu (also Mn and Ce) has reactivity for the the removal of Hg^0, respectively. 2%CuOx-10%CoOx/AC_N catalytic materials was optimized for the ability of removal CO and Hg^0 under simulative flue gas. Compared with other transition metal doping, Cu doped CoOx/AC_N had the improved catalytic ability for CO oxidation and Hg^0 removal. The calcination temperature greatly affects the existent form and valence state of CoOx with different redox properties resulting in the significant difference for CO oxidation. The coexistence of complex oxides including CuO, Cu_2O, Co_3O_4, Co_2O_3 and CoO would likely be beneficial to the simultaneous catalytic oxidation of CO and Hg^0, benefiting from the synergistic catalysis during the electro-interaction between Co and Cu cations. The removal of Hg° followed the adsorption process and also the catalytic oxidation reaction via Langmuir-Hinshelwood mechanism while the catalysis of CO abided by the Mars-van Krevelen mechanism with lattice oxygen species.

Acknowledgments

This work was financially supported by the National Key R&D Program of China(No. 2017YFC0210303), the National Natural Science Foundation of China (Nos. 21806009, 21677010), the China Postdoctoral Science Foundation (No. 2018M631344), and the Fundamental Research Funds for the Central Universities (Nos. 06500152, FRF-TP-18-019A1).

REFERENCE

Arena, F., Di Chio, R., Filiciotto, L., Trunfio, G., Espro, C., Palella, A., et al., 2017. Probing the functionality of nanostructured MnCeOx catalysts in the carbon monoxide oxidation. Appl. Catal. B 218, 803–809.

Chen, C., Jia, W., Liu, S., Cao, Y., 2018a. The enhancement of CuO modified V_2O_5-WO_3/TiO_2 based SCR catalyst for Hg^0 oxidation in simulated flue gas. Appl. Surf. Sci. 436, 1022–1029.

Chen, G., Xu, Q., Wang, Y., Song, G., Li, C., Zhao, W., et al., 2016. Solubility product difference-guided synthesis of Co_3O_4–CeO_2 core–shell catalysts for CO oxidation. Catal. Sci. Technol. 6, 7273–7279.

Chen, J., Li, C., Li, S., Lu, P., Gao, L., Du, X., et al., 2018b. Simultaneous removal of HCHO and elemental mercury from flue gas over Co-Ce oxides supported on activated coke impregnated by sulfuric acid. Chem. Eng. J. 338, 358–368.

Chi, G., Shen, B., Yu, R., He, C., Zhang, X., 2017. Simultaneous removal of NO and Hg^0 over Ce-Cu modified V_2O_5/TiO_2 based commercial SCR catalysts. J. Hazard. Mater. 330, 83–92.

Cimino, S., Scala, F., 2016. Removal of elemental mercury by MnOx catalysts supported on TiO_2 or Al_2O_3. Ind. Eng. Chem. Res. 55, 5133–5138.

Collins, S., Finos, G., Alcántara, R., del Rio, E., Bernal, S., Bonivardi, A., 2010. Effect of gallia doping on the acid–base and redox properties of ceria. Appl. Catal. A 388, 202–210.

Davó-Quiñonero, A., Lozano-Castelló, D., Bueno-López, A., 2017. Unexpected stability of CuO/cryptomelane catalyst under preferential oxidation of CO reaction conditions in the presence of CO_2 and H_2O. Appl. Catal. B 217, 459–465.

Fu, K-L., Yao, M-Y., Qin, C-g., Cheng, G-W., Li, Y., Cai, M., et al., 2016. Study on the removal of oxidized mercury (Hg^{2+}) from flue gas by thiol chelating resin. Fuel Process. Technol 148, 28–34.

Gao, F., Chu, C., Zhu, W., Tang, X., Yi, H., Zhang, R., 2019a. High-efficiency catalytic oxidation of nitric oxide over spherical Mn-Co spinel catalyst at low temperature. Appl. Surf. Sci. 479, 548–556.

Gao, F., Tang, X., Yi, H., Zhang, B., Zhao, S., Wang, J., et al., 2018a. NiO-modified coconut shell based activated carbon pretreated with KOH for the high-efficiency adsorption of NO at ambient temperature. Ind. Eng. Chem. Res. 57, 16593–16603.

Gao, F., Tang, X., Yi, H., Zhao, S., Wang, J., Gu, T., 2019b. Improvement of activity, selectivity and H_2O&SO_2-tolerance of micro-mesoporous $CrMn_2O_4$ spinel catalyst for low-temperature NH_3-SCR of NOx. Appl. Surf. Sci. 466, 411–424.

Gao, F., Tang, X., Yi, H., Zhao, S., Wang, J., Shi, Y., et al., 2018b. Novel Co– or Ni–Mn binary oxide catalysts with hydroxyl groups for NH_3–SCR of NOx at low temperature. Appl. Surf. Sci. 443, 103–113.

Gao, F., Tang, X., Yi, H., Zhao, S., Zhu, W., Shi, Y., 2020. Mn_2NiO_4 spinel catalyst for high-efficiency selective catalytic reduction of nitrogen oxides with good resistance to H_2O and SO_2 at low temperature. J. Environ. Sci. 89, 145–155.

Gu, D., Jia, C-J., Bongard, H., Spliethoff, B., Weidenthaler, C., Schmidt, W., et al., 2014. Ordered mesoporous Cu–Ce–O catalysts for CO preferential oxidation in H_2-rich gases: Influence of copper content and pretreatment conditions. Appl. Catal. B 152–153, 11–18.

Guo, Y., Yan, N., Liu, P., Yang, S., Wang, J., Qu, Z., 2012. Removal of elemental mercury with Mn/Mo/Ru/Al_2O_3 membrane catalytic system. Front. Environ. Sci. Eng. 7, 464–473.

Han, L., He, X., Yue, C., Hu, Y., Li, L., Chang, L., et al., 2016. Fe doping Pd/AC sorbent efficiently improving the Hg^0 removal from the coal-derived fuel gas. Fuel 182, 64–72.

He, C., Shen, B., Chi, G., Li, F., 2016. Elemental mercury removal by CeO_2/TiO_2-PILCs under simulated coal-fired flue gas. Chem. Eng. J. 300, 1–8.

Huang, W-J., Xu, H-M., Qu, Z., Zhao, S-J., Chen, W-M., Yan, N-Q., 2016. Significance of Fe_2O_3 modified SCR catalyst for gas-phase elemental mercury oxidation in coal-fired flue gas. Fuel Process. Technol. 149, 23–28.

Jampaiah, D., Ippolito, J., S., Sabri, Y., Tardio, J., Selvakannan, P, R., Nafady, A., et al., 2016. Ceria-zirconia modified MnOx catalysts for gaseous elemental mercury oxidation and adsorption. Catal. Sci. Technol. 6, 1792–1803.

Jansson, J., Palmqvist, AEC., Fridell, E., Skoglundh, M., Österlund, L., Thormählen, P., et al., 2002. On the catalytic activity of Co_3O_4 in low-temperature CO oxidation. J. Catal. 211, 387–397.

Jew, AD., Rupp, EC., Geatches, DL., Jung, J-E., Farfan, G., Bahet, L., et al., 2015. Mercury Interaction with the fine fraction of coal-combustion fly ash in a simulated coal power plant flue gas stream. Energ. Fuel. 29, 6025–6038.

López-Antón, MA., Fernandez, N., Martínez-Tarazona, M., 2016. The application of regenerable sorbents for mercury capture in gas phase. Environ. Sci. Pollut. Res. Int. 23, 24495–24503.

Li, L., He, Y., Lu, X., 2017. New insights into mercury removal mechanism on CeO_2-based catalysts: a first-principles study. Front. Environ. Sci. Eng. 12, 1–9.

Liu, C., Gong, L., Lu, M., Sun, T., Dai, R., Liu, Q., et al., 2017a. The solid-state-grinding synthesis of maganese-modified cobalt oxides and application in the low-temperature CO preferential oxidation in H_2-rich gases. Catal. Surv. Asia. 21, 175–184.

Liu, P., Li, T., Chen, H., Hensen, E.J.M., 2017b. Optimization of Au^0–Cu^+ synergy in Au/$MgCuCr_2O_4$ catalysts for aerobic oxidation of ethanol to acetaldehyde. J. Catal. 347, 45–56.

Meng, D., Xu, Q., Jiao, Y., Guo, Y., Guo, Y., Wang, L., et al., 2018. Spinel structured Co_aMn_bOx mixed oxide catalyst for the selective catalytic reduction of NOx with NH_3. Appl. Catal. B 221, 652–663.

Penkala, B., Gatla, S., Aubert, D., Ceretti, M., Tardivat, C., Paulus, W., et al., 2018. In situ generated catalyst: copper(ii) oxide and copper(i) supported on $Ca_2Fe_2O_5$ for CO oxidation. Catal. Sci. Technol. 8, 5236–5243.

Ramesh, K., Chen, L., Chen, F., Liu, Y., Wang, Z., Han, Y-F., 2008. Re-investigating the CO oxidation mechanism over unsupported MnO, Mn_2O_3 and MnO_2 catalysts. Catal. Today 131, 477–482.

Song, Y., Liu, L., Fu, Z., Ye, Q., Cheng, S., Kang, T., et al., 2017. Excellent performance of Cu-Mn/Ti-sepiolite catalysts for low-temperature CO oxidation. Front. Environ. Sci. Eng. 11 (2) 5 (1-9 pages).

Stošić, D., Bennici, S., Rakić, V., Auroux, A., 2012. CeO_2–Nb_2O_5 mixed oxide catalysts: preparation, characterization and catalytic activity in fructose dehydration reaction. Catal. Today 192, 160–168.

Tang, X., Gao, F., Xiang, Y., Yi, H., Zhao, S., 2015. Low temperature catalytic oxidation of nitric oxide over the Mn–CoOx catalyst modified by nonthermal plasma. Catal. Commun. 64, 12–17.

Wang, F., Wang, S., Zhang, L., Yang, H., Gao, W., Wu, Q., et al., 2016. Mercury mass flow in iron and steel production process and its implications for mercury emission control. J. Environ. Sci. 43, 293–301.

Wang, Y-Z., Zhao, Y-X., Gao, C-G., Liu, D-S., 2007. Preparation and catalytic performance of Co_3O_4 catalysts for low-temperature CO oxidation. Catal. Lett. 116, 136–142.

Wang, Y., Wang, Y., Li, X., Liu, Z., Zhao, Y., 2018. Effect of ultrasonic treatment of palygorskite on the catalytic performance of Pd-Cu/palygorskite catalyst for room temperature CO oxidation in humid circumstances. Environ. Technol. 39, 780–786.

Xiang, W., Liu, J., Chang, M., Zheng, C., 2012. The adsorption mechanism of elemental mercury on CuO (110) surface. Chem. Eng. J. 200–202, 91–96.

Xie, Y., Li, C., Zhao, L., Zhang, J., Zeng, G., Zhang, X., et al., 2015. Experimental study on Hg^0 removal from flue gas over columnar MnOx-CeO_2/activated coke. Appl. Surf. Sci. 333, 59–67.

Xu, W., Shao, M., Yang, Y., Liu, R., Wu, Y., Zhu, T., 2017. Mercury emission from sintering process in the iron and steel industry of China. Fuel Process. Technol. 159, 340–344.

Xu, W., Wang, H., Zhou, X., Zhu, T., 2014. CuO/TiO_2 catalysts for gas-phase Hg^0 catalytic oxidation. Chem. Eng. J. 243, 380–385.

Yi, Y., Li, C., Zhao, L., Du, X., Gao, L., Chen, J., et al., 2018. The synthetic evaluation of CuO-MnOx-modified pinecone biochar for simultaneous removal formaldehyde and elemental mercury from simulated flue gas. Environ. Sci. Pollut. Res. 25, 4761–4775.

Zhang, C., Chen, T., Liu, H., Chen, D., Xu, B., Qing, C., 2018. Low temperature SCR reaction over nano-structured Fe-Mn oxides: characterization, performance, and kinetic study. Appl. Surf. Sci. 457, 1116–1125.

Zhang, Q., Qiu, C., Xu, H., Lin, T., Lin, Z., Gong, M., et al., 2011. Low-temperature selective catalytic reduction of NO with NH_3 over monolith catalyst of MnOx/CeO_2–ZrO_2–Al_2O_3. Catal. Today 175, 171–176.

Zhang, R., Lu, K., Zong, L., Tong, S., Wang, X., Zhou, J., et al., 2017a. Control synthesis of CeO_2 nanomaterials supported gold for

catalytic oxidation of carbon monoxide. Mol. Catal. 442, 173–180.
Zhang, X-m., Deng, Y-Q., Tian, P., Shang, H-h., Xu, J., Han, Y-F., 2016a. Dynamic active sites over binary oxide catalysts: In situ/operando spectroscopic study of low-temperature CO oxidation over MnOx-CeO_2 catalysts. Appl. Catal. B 191, 179–191.
Zhang, X., Cheng, S., Zhang, W., Zhang, C., E Drewett, N., Wang, X., et al., 2017b. Mechanistic Insight into nano-architected Ag/Pr_6O_{11} catalysts for efficient CO oxidation. Ind. Eng. Chem. Res. 56, 11042–11048.
Zhang, X., Dong, H., Zhao, D., Wang, Y., Wang, Y., Cui, L., 2016b. Effect of support calcination temperature on Ag structure and catalytic activity for CO oxidation. Chem. Res. Chin. U. 32, 455–460.
Zhang, Y., Wang, A., Huang, Y., Xu, Q., Yin, J., Zhang, T., 2012. Nanocasting synthesis of mesostructured Co_3O_4 via a supercritical CO_2 deposition method and the catalytic performance for CO oxidation. Catal. Lett. 142, 275–281.
Zhao, B., Yi, H., Tang, X., Li, Q., Liu, D., Gao, F., 2016. Copper modified activated coke for mercury removal from coal-fired flue gas. Chem. Eng. J. 286, 585–593.
Zhao, B., Yi, HH., Tang, XL., Li, Q., Liu, D., Gao, F., 2019. Using CuO-MnOx/AC-H as catalyst for simultaneous removal of Hg degrees and NO from coal-fired flue gas. J. Hazard. Mater. 364, 700–709.
Zhao, Z., Bao, T., Li, Y., Min, X., Zhao, D., Muhammad, T., 2014. The supported CeO_2/Co_3O_4–MnO_2/CeO_2 catalyst on activated carbon prepared by a successive-loading approach with superior catalytic activity and selectivity for CO preferential oxidation in H_2-rich stream. Catal. Commun. 48, 24–28.
Zuo, Y., Yi, H., Tang, X., Zhao, S., Zhang, B., Wang, Z., et al., 2015. Study on active coke-based adsorbents for SO_2 removal in flue gas. J. Chem. Technol. Biotechnol. 90, 1876–1885.